2022 44th Annual International Conference of
the IEEE Engineering in Medicine & Biology Society (EMBC)
Scottish Event Campus, Glasgow, UK, July 11-15, 2022

2022 44th Annual International Conference of the IEEE Engineering in Medicine & Biology Society (EMBC) | 978-1-7281-2782-8/22/$31.00 ©2022 IEEE | DOI: 10.1109/EMBC48229.2022.9871073

Design, Fabrication and Performance Assessment of Flexible, Microneedle–Based Electrodes For ECG Signal Monitoring

Om Prakash Singh, Andrea Bocchino, Theo Guillerm and Conor O'Mahony, *Senior Member, IEEE*

***Abstract*— Microneedle-based electrodes have attracted significant attention for the monitoring of physiological signals, including ECG, EMG, and EOG, as they have the potential to eliminate the skin preparation and stability issues associated with conventional wet gel electrodes. This paper describes the development of a polymeric flexible microneedle electrode (FMNE) that does not require skin abrasion and can be used for long-term ECG monitoring. Fabricated using a combination of epoxy resin microneedles bonded to a flexible substrate, the performance of the FMNE was compared to that of a conventional wet-gel electrode by simultaneously capturing the ECG signal using both electrodes, and estimating the signal-to-noise ratio (SNR) of each. Results show that the flexible electrode can acquire ECG signals in which all the characteristic components of the wave are visible, and that are comparable in quality to those obtained using commercial wet electrodes. Bland-Altman plots were drawn to validate the performance of FMNE, and show that the mean difference ± standard deviation in SNR obtained using wet electrodes and FMNE was 0.9 ± 0.7 dB.**

***Clinical Relevance*— These microneedle-based 'dry electrodes' could be used in long-term monitoring of biopotential activity.**

I. Introduction

Electrical activity in the heart, muscles brain and stomach generates characteristic signals referred to as an electrocardiogram (ECG), surface electromyogram (sEMG), electroencephalogram (EEG), and electrogastrogram (EGG), respectively. These signals may be used to perform a myriad of diagnostic procedures, and are widely acquired via self-adhesive electrodes affixed to the body [1]. An electrolytic gel is commonly used between electrode and skin to reduce the influence of the high-impedance stratum corneum (SC) layer and to enhance the quality of the signal as depicted in Figure 1(a). However, this gel may cause allergic reactions and skin irritations and tends to dry out over time; as a result, these wet gel electrodes cannot be used for lengthy diagnostic procedures.

To eradicate the need for gel application, dry electrodes are proposed [2], however, the SC layer must be removed to reduce the skin-electrode impedance and to increase signal-to-noise ratio (SNR). Alternatively, electrodes consisting of arrays of short, sharp microneedles could address this problem by painlessly penetrating the SC layer and making direct contact to the underlying epidermal layers, Figure 1(b). The penetration process is minimally invasive and can avoid allergic reactions and skin irritations, and, since electrolytic gel is not required, electrically conductive microneedles are expected to provide a stable skin-electrode interface for use in long-term monitoring procedures.

However, most microneedle are based on inflexible substrates that are do not conform well to human skin. In contrast, flexible microneedle electrodes (FMNE) could mechanically couple with the uneven structure of human skin, offer robust contact, and decrease motion-induced signal distortions.

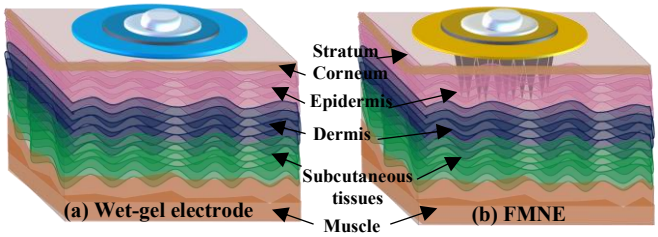

Figure 1. Skin interface with: (a) wet-gel electrode; and (b) flexible microneedle electrode (FMNE) using flexible and breathable substrate.

Microneedle array fabrication techniques include micromoulding [3,4], laser machining [5], lithography and etching [6,7], thermal drawing [8], magnetization-induced self-assembling [9], and 3D printing [10]. Most microneedle arrays are fabricated using a rigid substrate, in materials such as silicon, copper, poly lactic-co-glycolic acid, polymethyl methacrylate, and stainless steel. Recent works have begun to investigate the development of flexible microneedle electrodes: Kim *et al.* [4] fabricated a flexible band-integrated curved microneedle electrode using a micromoulding process, but its curved substrate was rigid. Wang *et al.* [11] proposed a flexible parylene-based microneedle electrode for long-term monitoring of biological signals, but which required the use of a complex fabrication process. Ren *et al.* [8] reported a microneedle electrode with flexible polyethylene terephthalate

This work was funded by the Government of Ireland through the Disruptive Technologies Innovation Fund, Grant DT2018 0291-A (HOLISTICS).

Conor O'Mahony is with the Tyndall National Institute, University College Cork, Lee Maltings, Dyke Parade, Cork T12 R5CP, Ireland (+353 21 234 6200; e-mail: conor.omahony@tyndall.ie).

Om Prakash Singh is with the Tyndall National Institute, University College Cork, Lee Maltings, Dyke Parade, Cork T12 R5CP, Ireland (e-mail: omprakash.singh@tyndall.ie)

Andrea Bocchino is with the Tyndall National Institute, University College Cork, Lee Maltings, Dyke Parade, Cork T12 R5CP, Ireland (e-mail: andrea.bocchino@tyndall.ie)

Theo Guillerm is with the Tyndall National Institute, University College Cork, Lee Maltings, Dyke Parade, Cork T12 R5CP, Ireland (e-mail: theo.guillerm@tyndall.ie)

substrate for wearable bio-signal monitoring, using a laser-direct writing and magneto-rheological drawing lithography process that may be challenging to use in mass manufacture. Recently, Lozano and Stoeber [12] presented a polymeric FMNE for biosignals monitoring, employing multiple resin and production processing steps.

This study aimed to develop a polymeric FMNE based around the use of a micromoulding process and flexible substrate. The performance of the FMNE with respect to a conventional wet-gel electrode was estimated by simultaneously recording ECG signals using both electrodes, and quantifying the SNR of each. Bland-Altman (B&A) plots were drawn to show that the performance of the FMNE was comparable to that of wet gel electrodes, but without the use of gel or skin abrasion. Excellent flexibility and reliability was also observed.

II. Materials and Methods

A. Overview of FMNE fabrication process

The process for fabrication of FMNE was adapted from [13] and shown in Figure 2. Potassium hydroxide (KOH) wet-etching [14] was first employed to fabricate master templates consisting of 100 mm diameter wafers of 500 µm tall silicon microneedles, which have a height:base diameter aspect ratio of 3:2, a tip radius of 50-100 nm and needle-to-needle pitch of 1750 µm.

The master template was then glued to a customised holder machined from polyvinyl chloride (PVC). A negative copy was prepared using Sylgard® 184 PDMS (Dow Corning, MI, USA) as depicted in Figure 2 (a), which acts as a front mould to create the microneedle surface. A second, back side, master was also fabricated using a PVC petri dish into which a custom geometry was milled. This master was intended to divide the wafer into individual circular electrodes, and was used to produce a second PDMS mould, Figure 2 (b). PDMS was polymerized by mixing pre-polymer with curing agent in a 10:1 ratio, followed by degassing at room temperature for 90 minutes. Finally, the polymerized moulds were baked at 80^0C for 2 hours.

Figure 2 (c) shows the process for the fabrication of solid MNAs using EPO-TEK 353ND epoxy resin (Epoxy Technology, MA, USA). The epoxy resin was mixed in 10:1 and poured onto the front mould to fill the needle tips, followed by degassing for 10-15 minutes.

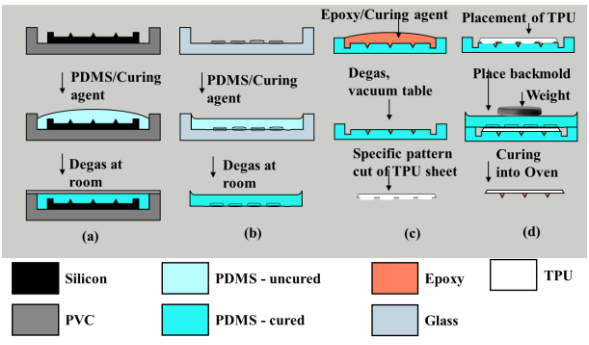

Figure 2. Overview of FMNE fabrication steps: (a) fabrication of front side, negative microneedle mould; (b) fabrication of back side mould; (c) fabrication of microneedle arrays using epoxy resin and cutting of TPU sheet using Cricut machine; (d) bonding of microneedle arrays with flexible TPU.

A 130 µm thick TPU sheet (ST604, Bemis Associates, Inc.) was used as a flexible and stretchable substrate. The TPU sheet was cut using a desktop cutting tool (Cricut, UT, USA), in patterns that defined the electrode shape and that matched the rear PDMS mould, Figure 2 (c). Then, the cut TPU substrate was placed over the epoxy-filled front mould, followed by the back side mould and a weight, Figure 2 (d). The stack was cured in an oven at 80^0C for one hour that allowed the bonding of microneedles with TPU. Figure 3 depicts (a) a TPU sheet cut to specific shape and size; (b) epoxy microneedles bonded with TPU.

B. Microneedle coating

Both the faces of FMNE were uniformly coated with a 20 nm thick titanium (Ti) adhesion layer, followed by a 100 nm thick layer of platinum (Pt) via sputtering.

C. Assembling of Electrodes

The electrodes were detached from wafers using a scalpel. The detached electrodes were attached to a conventional electrode (Red Dot Monitoring Electrodes, 3M, Ireland) from which the electrolytic gel was removed, using a biocompatible conductive epoxy (MED-H20E, Epoxy Technology Inc., Billerica, MA, USA). Assembled electrodes were sterilised under UV-Ozone (ProCleaner Plus, BioForce Nanoscience, UT, USA) for 5 minutes and packed into a plastic cover for storage purposes.

D. Performance assessment

The performance of the assembled electrodes was assessed by recording the ECG signal from one subject aged 35 years at room temperature in static conditions. The ECG signals were simultaneously recorded from both FMNE and standard wet-gel electrodes using a customized ECG acquisition board as presented in Figure 4. An Agilent E48980A LCR meter and customized LabVIEW software that limited the current as per the IEC60601-1 electrical safety standard was used to measure the skin-electrode impedance from the subject's forearm using a two-electrode system.

During recording, the subject was advised to sit in a chair in a relaxed position while wearing the electrodes; ECG signals were recorded for 2 minutes using a Bluetooth-enabled laptop. The study protocol was approved by the Clinical Research Ethics Committee of the Cork Teaching Hospitals (ECM 3 (ZZ) 10/11/20), and written informed consent was obtained from the participant.

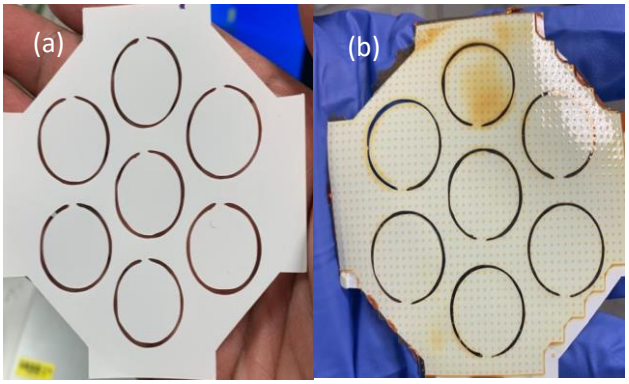

Figure 3. (a) TPU sheet cut using Cricut machine; (b) Epoxy microneedles bonded to TPU. The needles are visible as orange dots.

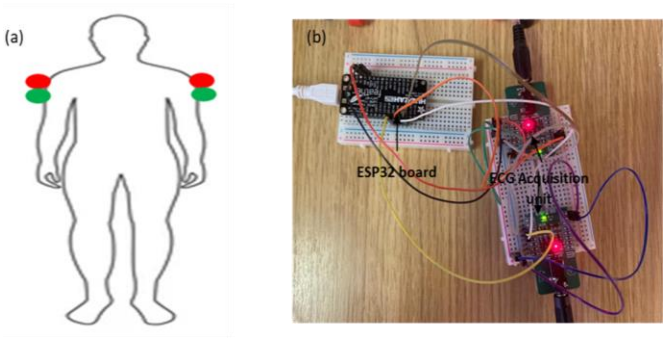

Figure 4. (a) Electrode position scheme for the acquisition of ECG signal from both FMNE dry (solid red circle) and wet-gel electrodes (light green solid circle) [15]; (b) The ECG acquisition set-up includes two MAX86150 ECG acquisition boards, integrated with an ESP32 board.

SNR was estimated using Equation (1) to assess the quality of the signal obtained from both electrodes.

$$snr_{dB} = 20 \times log_{10} \frac{A_{pp}^{signal}}{A_{pp}^{noise}} \quad , \qquad (1)$$

where A_{pp}^{signal} and A_{pp}^{noise} represent the peak-to-peak ADC counts of the QRS wave and noise in the isoelectric region between the T and P waves, respectively.

The signal-processing algorithm for the quantification of SNR was performed using Labview. Further, the performance of both the electrodes was validated by drawing a B&A plot using MATLAB R2019b.

III. Results and Discussions

Figure 5 displays the front and rear surfaces of a metalized wafer, consisting of seven detachable electrodes. Each electrode comprises more than 120 microneedles. A uniform layer of platinum on the MNA bonded TPU was achieved by sputtering. SEM was performed to characterize the FMNE sample surface morphology and sharpness of the microneedle tips. Figure 6 (a) and (b) depict the array of microneedles and sharpness of the tip (~11 µm radius), respectively. The tip was found to be sharp enough to pierce the upper layer of skin.

Figure 7 demonstrates the electrode flexibility. We observed that there was no sign of separation of TPU substrate from the epoxy and supportive layer as well. In addition, there was no breakage of microneedles observed during use. Figure 8 depicts the assembled electrode after sterilization.

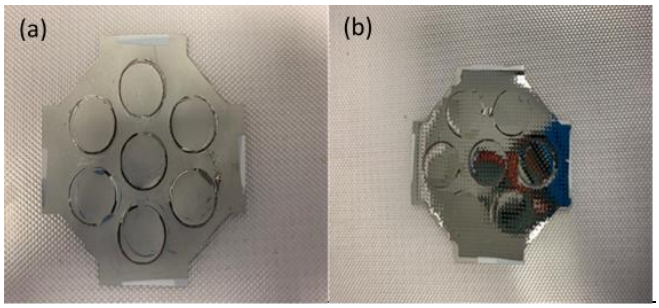

Figure 5. (a) Left: platinum-coated back side of FMNE wafer. (b) Right: platinum coated front side of FMNE wafer.

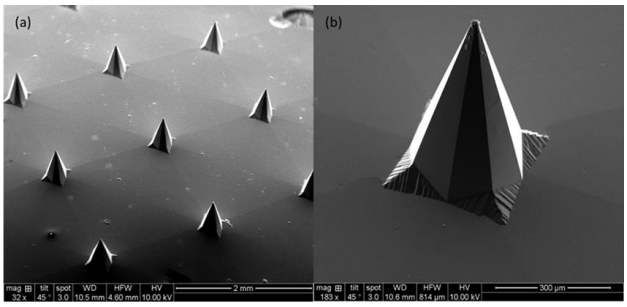

Figure 6. (a) 500µm tall microneedle polymeric microneedle array, captured with tilted 45^0 angle; (b) 500µm tall microneedle polymeric microneedle.

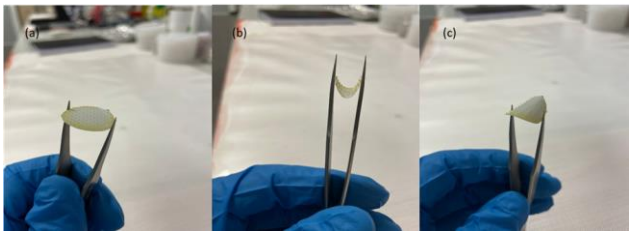

Figure 7. (a) Top left: tweezer used to hold the samples; (b) Top centre: bending in inward direction; (b) Top right: bending in outward direction.

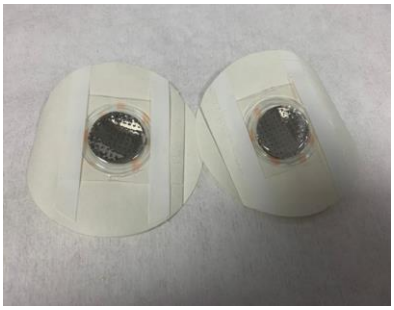

Figure 8. Assembled MNA based flexible electrodes

A. Performance assessment using ECG signal

ECG signals were simultaneously recorded using both FMNE and wet-gel electrodes in static conditions for 2 minutes from one subject. The recorded ECG signals are very similar to those obtained from standard wet-gel electrodes, and typical cardiac signatures P, QRS, and T waves are visible as shown in Figure 9. 20 segments were extracted from the 2-minute signal, each of which comprised a minimum of 10 R peaks. The SNR was estimated for each peak. An average SNR value was determined for each segment and a B&A plot was drawn to help in identifying any systematic differences between the wet-gel and FMNE electrodes.

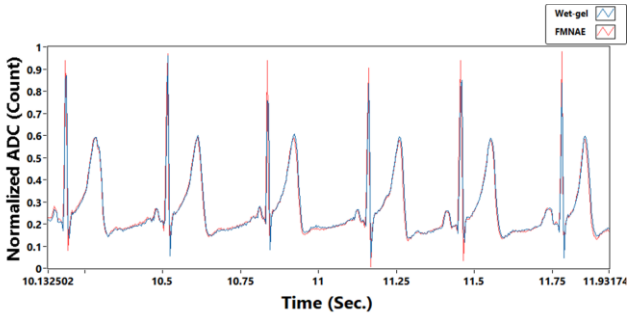

Figure 9. Illustration of recorded ECG signal using wet-gel and FMNE electrodes.

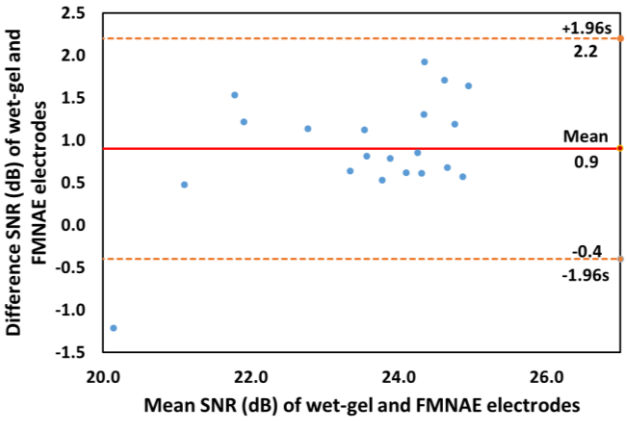

Figure 10. Bland-Altman plot of SNR difference against mean SNR for each measurement. The mean difference is 0.9dB; the dotted lines represent the upper and lower limits of agreement.

The SNR values were calculated as 23.1 ± 1.2 dB and 24.0 ± 1.5 dB for the FMNE and wet gel electrodes, respectively. B&A plotting provides two key parameters, namely, bias and limit of agreement, which are utilized to assess the precision of the FMNE. The bias value indicates the mean difference between electrode measurements. The limits of agreement, defined as ±1.96 SD, indicate the range within which 95% of the differences between future measurements are presumed to lie.

From Figure 10, it can be observed that the lower and upper limits of SNR of the wet-gel and FMNE electrodes were -0.4 dB and 2.2 dB, respectively. The (mean difference ± standard deviation) value was 0.9 ± 0.7 dB, which indicates that the performance of the FMNE electrodes is comparable to that of the wet-gel electrodes. It should also be noted that the 95% agreement limits were from -1.97% to 9.51%, which is within the value of ±10% that has been reported as an acceptable limit for electrode performance when assessed against reference standards [16]. Although ECG bandwidth typically ranges from 0.05 Hz to 150 Hz, skin-electrode impedance was measured from 20 Hz to 1000 Hz due to equipment limitations. Hence, the frequency was swept from 20 Hz to 1000 Hz, with an interval of 100 Hz. The impedance measured at 20 Hz by FMNE and gel electrodes was 75 kΩ and 79 kΩ respectively. However, this does not address the subject-to-subject variations of skin-electrode impedance [17].

IV. Conclusions

This study presents a microneedle-based electrode using a flexible substrate, and fabricated via a micromoulding process that could be effective in mass production of electrodes in low cost and high volume. This approach simplifies the process, reduces the time, and requires less material in the fabrication of an FMNE than that reported in our previous work [14]. The performance of electrodes was assessed by simultaneously recording the ECG signal from both FMNE and commercial wet electrodes, and using Bland-Altman analysis. The B&A plot reveals that the mean difference in SNR was 0.9 ± 0.7 dB. Hence, the FMNE has the potential to acquire ECG signals comparable in quality to those of commercial wet electrodes, but without the use of skin abrasion or wet gel.

In this case, the performance of the electrodes was evaluated by recording the ECG signal in static conditions from one subject. However, future research will focus on assessing electrodes with an increased number of subjects in both static and dynamic conditions, and by measuring different biological signals such as EMG and EEG. Additional biomechanical and reliability analysis is also ongoing.

Acknowledgment

We would like to thank Marisa Phelen at Henkel Ireland for providing the TPU substrate materials.

References

[1] N. V. Thakor, "Biopotentials and electrophysiology measurement. Measurement, Instrumentation, and Sensors," Handbook J G Webster (Boca Raton, FL:CRC Press), pp.64-1, 2017.

[2] K.F. Wu, and Y.T. Zhang, "Contactless and continuous monitoring of heart electric activities through clothes on a sleeping bed," In 2008 *Proc. Int. Conf. Inf. Technol,* pp. 282-285.

[3] M.Arai,Y.Nishinaka, and N. Miki, "Long-term electroencephalogram measurement using polymer-based dry microneedle electrode,". In 2015 *Int. Conf. Solid-State Sens. Actuators Microsyst*, pp. 81-84.

[4] M.Kim, T. Kim, D.S. Kim, and W.K.Chung, "Curved microneedle array-based sEMG electrode for robust long-term measurements and high selectivity," *Sensors*, vol. 15, no. 7, pp.16265-16280, Jul 2015.

[5] W. Zhou, W.S. Ling, W. Liu, Y. Peng, J. Peng, "Laser direct micromilling of copper-based bioelectrode with surface microstructure array," *Opt. Lasers Eng.* vol. 73, pp. 7–15,Oct 2015.

[6] R.Wang, X.Jiang, W.Wang, and Z. Li, "A microneedle electrode array on flexible substrate for long-term EEG monitoring," *Sens Actuators B Chem*, vol. 244, pp.750-758, Jun 2017.

[7] C. O'Mahony, F. Pini, A. Blake, C. Webster, J. O'Brien, and K.G. McCarthy, "Microneedle-based electrodes with integrated through-silicon via for biopotential recording," *Sens. Actuator A Phys.*,vol. 86, pp.130-136, Oct 2012.

[8] L. Ren, Q. Jiang, K. Chen, Z. Chen, C. Pan, and L. Jiang, "Fabrication of a micro-needle array electrode by thermal drawing for bio-signals monitoring," *Sensors*, vol. 16, no. 6, p.908, Jun 2016.

[9] C. Pan, K. Chen, L. Jiang, Z. Chen, L. Ren, L. Liang, and W. Yuan, "Magnetization-induced self-assembly method: Micro-needle array fabrication," *J. Mater. Process. Technol.*, vol. 227, pp.251-258, Jan 2016.

[10] P. Salvo, R. Raedt, E. Carrette, D. Schaubroeck, J. Vanfleteren, and L. Cardon, "A 3D printed dry electrode for ECG/EEG recording," *Sens. Actuator A Phys.*, vol. 174, pp.96-102, Feb 2012.

[11] L. Ren, Q. Jiang, Z. Chen, K. Chen, S. Xu, J. Gao, and L. Jiang, "Flexible microneedle array electrode using magnetorheological drawing lithography for bio-signal monitoring," Sens. Actuator A Phys., vol. 268, pp.38-45, Dec 2017.

[12] J. Lozano, and B.Stoeber, "Fabrication and characterization of a microneedle array electrode with flexible backing for biosignal monitoring," *Biomed. Microdevices*, vol. 23, no. 4, pp.1-19, Dec. 2021.

[13] N. Wilke, and A. Morrissey, "Silicon microneedle formation using modified mask designs based on convex corner undercut," *J. Micromech. Microeng*, vol. 17, no. 2, p.238, Dec 2006.

[14] C. O'Mahony, K. Grygoryev, A. Ciarlone, G. Giannoni, A. Kenthao, and P. Galvin, "Design, fabrication and skin-electrode contact analysis of polymer microneedle-based ECG electrodes," J. Micromech. Microeng, vol. 26, no. 8, p.084005, Jul 2016.

[15] O. Pahlm, and G.S. Wagner, "Proximal placement of limb electrodes: a potential solution for acquiring standard electrocardiogram waveforms from monitoring electrode positions," *J. Electrocardiol.*, vol. 41, no. 6, pp.454-457, Nov 2008.

[16] L.A. Critchley, and J.A. Critchley, "A meta-analysis of studies using bias and precision statistics to compare cardiac output measurement techniques," *J Clin Monit Comput*, vol. 15, no. 2, pp.85-91, Feb 1999 .

[17] M.A. Yokus, and J.S. Jur, "Fabric-based wearable dry electrodes for body surface biopotential recording," *IEEE. Trans. Biomed. Eng.*, vol. 63, no. 2, pp.423-430, Jul 2015.